Received: 4 January 2020 | Revised: 22 April 2020 | Accepted: 27 June 2020

DOI: 10.1002/cac2.12075

CANCER COMMUNICATIONS Open Access

ORIGINAL ARTICLE

The FTO/miR-181b-3p/ARL5B signaling pathway regulates cell migration and invasion in breast cancer

Yuanyuan Xu[1,*] | **Shuang Ye**[1,*] | **Nan Zhang**[1] | **Shuhui Zheng**[2] | **Huatao Liu**[3] | **Kewen Zhou**[1] | **Ling Wang**[1] | **Yue Cao**[4] | **Peng Sun**[5] | **Tinghuai Wang**[1]

[1] Department of Physiology, Zhongshan School of Medicine, Sun Yat-sen University, Guangzhou, Guangdong 510080, P. R. China

[2] Research Center for Translational Medicine, The First Affiliated Hospital of Sun Yat-sen University, Guangzhou, Guangdong 510080, P. R. China

[3] Department of Clinical Medicine, Zhongshan School of Medicine, Sun Yat-sen University, Guangzhou, Guangdong 510080, P. R. China

[4] Department of Basic Medicine, Zhongshan School of Medicine, Sun Yat-sen University, Guangzhou, Guangdong 510080, P. R. China

[5] Department of Pathology, State Key Laboratory of Oncology in South China, Collaborative Innovation Center for Cancer Medicine, Sun Yat-sen University Cancer Center, Guangzhou, Guangdong 510060, P. R. China

Correspondence
Tinghuai Wang, M.D. Department of Physiology, Zhongshan School of Medicine, Sun Yat-sen University, Guangzhou 510080, Guangdong, P. R. China.
Email: wangth@mail.sysu.edu.cn
Peng Sun, Ph.D. Department of Pathology, Sun Yat-sen University Cancer Center, State Key Laboratory of Oncology in South China, Collaborative Innovation Center for Cancer Medicine, Guangzhou 510060, Guangdong, P. R. China.
Email: sunpeng1@sysucc.org.cn

*Yuanyuan Xu and Shuang Ye contributed equally to this paper as co-first authors.

Abstract

Background: N6-methyladenosine (m^6A) RNA modification has been demonstrated to be a significant regulatory process in the progression of various tumors, including breast cancer. Fat mass and obesity-associated (FTO) enzyme, initially known as the obesity-related protein, is the first identified m^6A demethylase. However, the relationship between FTO and breast cancer remains controversial. In this study, we aimed to elucidate the role and clinical significance of FTO in breast cancer and to explore the underlying mechanism.

Methods: We first investigated the expression of FTO in breast cancer cell lines and tissues by quantitative reverse transcription-PCR (qRT-PCR), Western blotting, and immunohistochemistry. Wound healing assay and Transwell assay were performed to determine the migration and invasion abilities of SKBR3 and MDA-MB453 cells with either knockdown or overexpression of FTO. RNA sequencing (RNA-seq) was conducted to decipher the downstream targets of FTO. qRT-PCR,

Abbreviations: 3′ UTR, 3′ untranslated region; ARL, ADP ribosylation factor-like.; ARL5B, ADP ribosylation factor like GTPase 5B; ASB2, ankyrin repeat and SOCS box containing 2; BNIP3, BCL2 interacting protein 3; CCK-8, Cell Counting Kit-8; CLTA, clathrin light chain A; DFS, disease-free survival; DGCR8, DiGeorge syndrome critical region 8; DMEM, Dulbecco's modified Eagle medium; FBS, fetal bovine serum; FFPE, formalin-fixed; FTO, fat mass and obesity associated; GAPDH, glyceraldehyde-3-phosphate dehydrogenase; HE, hematoxylin and eosin; HER2, human epidermal growth factor receptor 2; IHC, immunohistochemistry; IRX3, iroquois homeobox 3; KEGG, Kyoto Encyclopedia of Genes and Genomes; m^6A, N6-methyladenosine; MA2, the ethyl ester form of meclofenamic acid; MeRIP-seq, methylated RNA immunoprecipitation sequencing; METTL14, methyltransferase like 14; METTL3, methyltransferase like 3; miRNA, microRNA; NIH, National Institutes of Health and the Laboratory; one-way ANOVA, one-way analysis of variance; OS, overall survival paraffin-embedded; PCMTD1, protein-L-isoaspartate (D-aspartate) O-methyltransferase domain containing 1; PVDF, polyvinylidene difluoride; qRT-PCR, quantitative reverse transcription-PCR; RAP2C, Ras-related protein Rap-2c; RARA, retinoic acid receptor alpha; RFS, recurrence-free survival; RIMKLB, ribosomal modification protein rimK like family member B; RNA-seq, RNA-sequencing; ROC, receiver operating characteristic; SDS-PAGE, sodium dodecyl sulfate-polyacrylamide gel electrophoresis; siRNA, small interfering RNA; SOWAHB, sosondowah ankyrin repeat domain family member B; STR, short tandem repeat; TCGA, The Cancer Genome Atlas Program

luciferase reporter assay, and Western blotting were employed to confirm the existence of the FTO/miR-181b-3p/ARL5B axis. The biological function of ADP ribosylation factor like GTPase 5B (ARL5B) in breast cancer cells was evaluated by wound healing assay and Transwell invasion assay.

Results: High FTO expression was observed in human epidermal growth factor receptor 2 (HER2)-positive breast cancer, predicting advanced progression (tumor size [$P < 0.001$], nuclear grade [$P = 0.001$], peritumoral lymphovascular invasion [$P < 0.001$), lymph node metastasis [$P = 0.002$], and TNM stage [$P = 0.001$]) and poor prognosis. Moreover, FTO promoted cell invasion and migration *in vitro*. Mechanistically, RNA-seq and further confirmation studies suggested that FTO up-regulated ARL5B by inhibiting miR-181b-3p. We further verified that ARL5B also displayed carcinogenic activity in breast cancer cells.

Conclusion: Our work demonstrated the carcinogenic activity of FTO in promoting the invasion and migration of breast cancer cells via the FTO/miR-181b-3p/ARL5B signaling pathway.

KEYWORDS

ARL5B, breast cancer, disease-free survival, Fat mass and obesity-associated (FTO) enzyme, human epidermal growth factor receptor 2, m6A modification, metastasis, miR-181b-3p, overall survival

1 | BACKGROUND

Breast cancer is the second leading cause of cancer-related deaths among women worldwide [1]. Novel interventions, including endocrine therapy, anti-human epidermal growth factor receptor 2 (HER2) targeted therapy, and immunotherapy, have strikingly improved the survival and clinical outcomes for patients with breast cancer. However, approximately 10%-41% of breast cancer patients experience distant recurrence after 5 years of endocrine therapy depending on the node status and grade of the primary tumor [2]. Metastatic breast cancer accounts for the majority of cancer-related deaths in women worldwide [3], and the 5-year survival rate drops to 25% once distant metastasis occurs [4]. Numerous studies have indicated that the posttranscriptional regulation process is extensively involved in tumor biology, evolution, and pathology [5, 6], and a better understanding of the specific oncogenes may reveal the molecular mechanisms involved in the metastasis and development of breast cancer.

N6-methyladenosine (m^6A) modification, with methylated adenosine at the N6 position, is the most abundant internal modification of eukaryotic mRNA and noncoding RNA [7]. Recent studies have illustrated the critical roles of m^6A modification in tissue development, stem cell self-renewal and differentiation, biological rhythm, and DNA damage repair [8, 9]. Fat mass and obesity-associated (FTO) protein, which was originally defined as an energy metabolism-related protein associated with increased body mass and obesity in children and adults [10], is the first identified m^6A demethylase it catalyzes m^6A demethylation in an Fe(II)- and α-ketoglutarate-dependent manner [11]. Recently, FTO was deemed an m^6A "eraser" and helped elucidate the involvement of posttranscriptional regulation by m^6A modification in complicated carcinogenic networks [12], including acute myeloid leukemia [13], glioblastoma [14], and breast cancer [15]. Although previous studies have shown that *FTO* gene polymorphisms were related to the incidence of breast cancer [16] and that some variations exerted their effects on breast cancer risk by regulating the iroquois homeobox 3 (IRX3) [17, 18], the impact of FTO, especially as an RNA demethylase, on breast cancer progression and metastasis remains poorly understood.

MicroRNAs (miRNAs) are a family of short non-coding single-stranded RNAs containing 19-22 nucleotides that promote the degradation or translation inhibition of mRNA by targeting specific mRNAs and forming RNA-induced silencing complexes [19]. Mounting studies have focused on m^6A involvement in miRNA alterations in cell malignant transformation and tumor progression [20]. Methyltransferase like 14 (METTL14) facilitates DiGeorge syndrome critical region 8 (DGCR8) recognition by adding m^6A modification to pri-miR-126, subsequently leading to the improvement of hepatic carcinoma [21]. Moreover, methyltransferase like 3 (METTL3) was confirmed to

accelerate miR-221/222 maturation in a similar way, resulting in the proliferation of bladder cancer cells [22]. A methylated RNA immunoprecipitation sequencing (MeRIP-seq) study showed that the steady-state levels of several miRNAs were affected by the knockdown of FTO and that a significant fraction of miRNAs contained m^6A sites [23]. However, whether the miRNA alterations induced by FTO are related to breast cancer metastasis has not yet been investigated.

Herein, we examined the expression and effect of FTO in breast cancer and further explored the underlying mechanism to offer novel insight into breast cancer pathogenesis.

2 | MATERIALS AND METHODS

2.1 | Patients and tumor tissues

Formalin-fixed, paraffin-embedded (FFPE) specimens of tumor and paired non-tumor tissues from 408 patients with HER2-positive breast cancer diagnosed between January 1, 2005 and December 31, 2013, along with patients' follow-up data, were collected from Sun Yat-sen University Cancer Center (Guangzhou, Guangdong, China). The inclusion criteria were as follows: (1) patients had pathologically diagnosed HER2-positive breast cancer (2) they underwent primary tumor resection after diagnosis and (3) their complete follow-up information was available. All follow-up information was collected and managed according to the rules of Sun Yat-sen University Cancer Center. The follow-up deadline was September 20, 2019. This study was approved by the Ethics Committee of Sun Yat-sen University Cancer Center. Written informed consent was signed by the involved patients to allow the use of their data in clinical researches.

2.2 | Immunohistochemistry (IHC)

All procedures were carried out as previously described [24]. The FFPE tissues mentioned above were sectioned into 5 μm-thick slides. For hematoxylin and eosin (HE) staining, slides were dewaxed and then stained with hematoxylin and eosin according to routine procedures. For IHC staining, the slides were deparaffinized, antigen retrieval was performed, and then the slides were blocked and processed consecutively. The slides were incubated with the primary antibody against FTO (1:500, #31687, Cell Signaling Technology, Inc., Danvers, MA, USA) or HER2 (1:100, #2242, Cell Signaling Technology). The staining was scored by two independent and experienced pathologists and calculated as the product of the staining intensity (0, negative; 1, weak; 2, moderate; and 3, strong staining) and percentage of positive cells (0, 0; 1, 1%-20%; 2, 21%-50%; 3, 51%-70%; 4, 71%-100%). The optimal cut-off value of FTO (8.0) generated from the receiver operating characteristic (ROC) curve divided FTO expression into high or low.

2.3 | Cell lines and culture

The human breast cancer cell lines MCF7, T47D, BT474, SKBR3, MDA-MB453, MDA-MB231, and BT549 and the immortalized mammary epithelial cell line MCF10A were purchased from the Institute of Biochemistry and Cell Biology, Shanghai Institute of Biological Sciences (Shanghai, China). The authenticity of all cell lines was confirmed by short tandem repeat (STR) DNA profiling analysis. Cells were cultured in Dulbecco's modified eagle medium (DMEM) (Sigma-Aldrich, Merck Millipore, Darmstadt, Germany) supplemented with 10% fetal bovine serum (FBS) (Gibco, Thermo Fisher Scientific, Inc., Waltham, MA, USA) in a humidified atmosphere at 37°C with 5% CO_2. Cancer cells subcultured for less than 5-6 times were used in all experiments.

2.4 | RNA and plasmid transfection

Small interfering RNAs (siRNAs) designed for FTO (siFTO) or ADP ribosylation factor like GTPase 5B (ARL5B) (siARL5B) and negative control siRNA (siCtrl) were obtained from RiboBio Co., Ltd. (Guangzhou, Guangdong, China). Plasmid clones expressing FTO (oeFTO), ARL5B (oeARL5B), or empty vector (oeVec) were purchased from Sino Biological Inc. (Beijing, China). All miR-181-3p mimics, inhibitors, and corresponding negative controls (miR-NC, miR-NC2) used for transfection were purchased from GenePharma Co., Ltd. (Shanghai, China). Transfection was conducted using Lipofectamine 3000 (Invitrogen, Thermo Fisher Scientific, Inc., Waltham, MA, USA) according to the manufacturer's instructions.

2.5 | RNA m^6A quantification

Total RNA was extracted using an RNeasy FFPE kit (Qiagen, Hilden, Germany) for tissues or TRIzol (Thermo Fisher Scientific, Inc.) for cells following the manufacturer's protocol. The relative m^6A content was measured by using the EpiQuik m^6A RNA Methylation Quantification kit (colorimetric) (EpiGentek Group Inc., Farmingdale, NY, USA). Briefly, 200 ng of qualified RNA was added to the assay wells provided by the kit. Capture antibody, detection antibody, and enhancer solution were sequentially added according to the manufacturer's instructions. Absorbance at 450 nm (A_{450}) was measured using a microplate reader (SpectraMax M5 Molecular Devices, LLC, Sunnyvale, CA, USA) to calculate the m^6A levels.

2.6 | Treatment with FTO inhibitor

FTO selective inhibitor, the ethyl ester form of meclofenamic acid (MA2) [25], was a gift from Professor Cai-Guang Yang (Chinese Academy of Sciences Key Laboratory of Receptor Research, Shanghai Institute of Materia Medical, Shanghai, China). A stock solution of MA2 (60 mmol/L) was dissolved in DMSO and stored at -20°C. After incubation with gradient concentrations of MA2 (40, 60, 80, and 100 μmol/L) for 48 h, SKBR3 and MDA-MB453 cells were collected for further studies. We found that MA2 at 80 μmol/L had the optimal inhibitory effect in the wound healing experiment. Therefore, 80 μmol/L MA2 was used for subsequent studies.

2.7 | Quantitative reverse transcription-PCR (qRT-PCR)

For mRNA or miRNA level examination, total RNA from tissues or cells was isolated by using the RNeasy FFPE kit or TRIzol. cDNA was synthesized using the PrimeScript RT reagent kit (Takara, Kusatsu, Japan), and the stem-loop RT primer method was applied in miRNA reverse transcription. qRT-PCR was performed using the SYBR-Green Master mix (Takara) in a CFX96 touch system (Bio-Rad Laboratories, Inc., Hercules, CA, USA). Glyceraldehyde-3-phosphate dehydrogenase (GAPDH) or U6 was used as an endogenous control for mRNA or miRNA detection, and the fold change was calculated with the relative quantification method ($2^{-\Delta\Delta Ct}$). Related primer sequences are listed in Supplementary Table S1.

2.8 | Western blotting

Briefly, breast cancer cells, after transfection or without processing, were harvested and lysed. Protein concentration was determined with the BCA protein assay kit (Thermo Fisher Scientific, Inc.). Equal amounts of protein were separated by 10% or 15% sodium dodecyl sulfate-polyacrylamide gel electrophoresis (SDS-PAGE) and transferred onto polyvinylidene difluoride (PVDF) membranes (Thermo Fisher Scientific, Inc.). Membranes were incubated with primary antibodies at 4°C overnight and then secondary antibodies at room temperature for 2 h. After washing, signals were detected using a Chemi-Doc™ imaging system (Bio-Rad Laboratories, Inc.). The following antibodies were purchased: anti-FTO (1:5000, #31687, Cell Signaling Technology), anti-ARL5B (1:1000, #CSB-PA002091GA01HU, Cusabio Technology LLC, Wuhan, Hubei, China), anti-GAPDH (1:5000, #BS60630, Bioworld Technology, Co, Ltd., Nanjing, Jiangsu, China), and anti-β-actin (1:5000, #BS-0061R, Santa Cruz Biotechnology Inc., Dallas, TX, USA) and secondary antibodies anti-rabbit IgG (#7074) and anti-mouse IgG (#7076) (1:5000, Cell Signaling Technology).

2.9 | Transwell assay

For the Transwell invasion assay, briefly, 5×10^4-1×10^5 cells in 200 μL serum-free DMEM were reseeded into the top of the insert of a Boyden chamber (Corning Inc., Corning, NY, USA) with 300 μg/mL Matrigel (BD Bioscience, San Jose, CA, USA), while 600 μL medium with 10% FBS was loaded into the well below. After 20-24 h incubation, invasive cells that passed through the filter were fixed with 0.1% paraformaldehyde (Solarbio Science & Technology Co., Ltd, Beijing, China) and stained with 0.1% crystal violet solution (Solarbio Science & Technology Co., Ltd). For the Transwell migration assay, all procedures were similar but without the incubation of Matrigel. The cells that passed through the filter were imaged at 100 × magnification in six random fields, and measured using the ImageJ software (National Institutes of Health and the Laboratory, Bethesda, MD, USA).

2.10 | Wound healing assay

As previously described [26], cultured cells were seeded into 24-well plates at a density of 2×10^5-4×10^5 cells per well. A 10 μL sterile pipette tip was used to scratch the cell layer and form a wound. The closure of the gap was imaged at designated time intervals under 100 × field, and the wound closure speed was evaluated using the ImageJ software.

2.11 | Cell viability assay

A total of 3000-6000 transfected cells were seeded into 96-well plates. At indicated time points, 10 μL of Cell Counting Kit-8 (CCK-8) reagent (Dojindo, Kumamoto, Japan) was added following the manufacturer's instructions. A_{450} was measured on a microplate reader (SpectraMax M5 Molecular Devices, LLC).

2.12 | RNA sequencing (RNA-seq)

RNA-seq was performed by RiboBio Co., Ltd. Total RNA from SKBR3 cells transfected with siFTO or siCtrl was extracted with TRIzol. RNA sequencing libraries were constructed using the TruSeq Small RNA Library

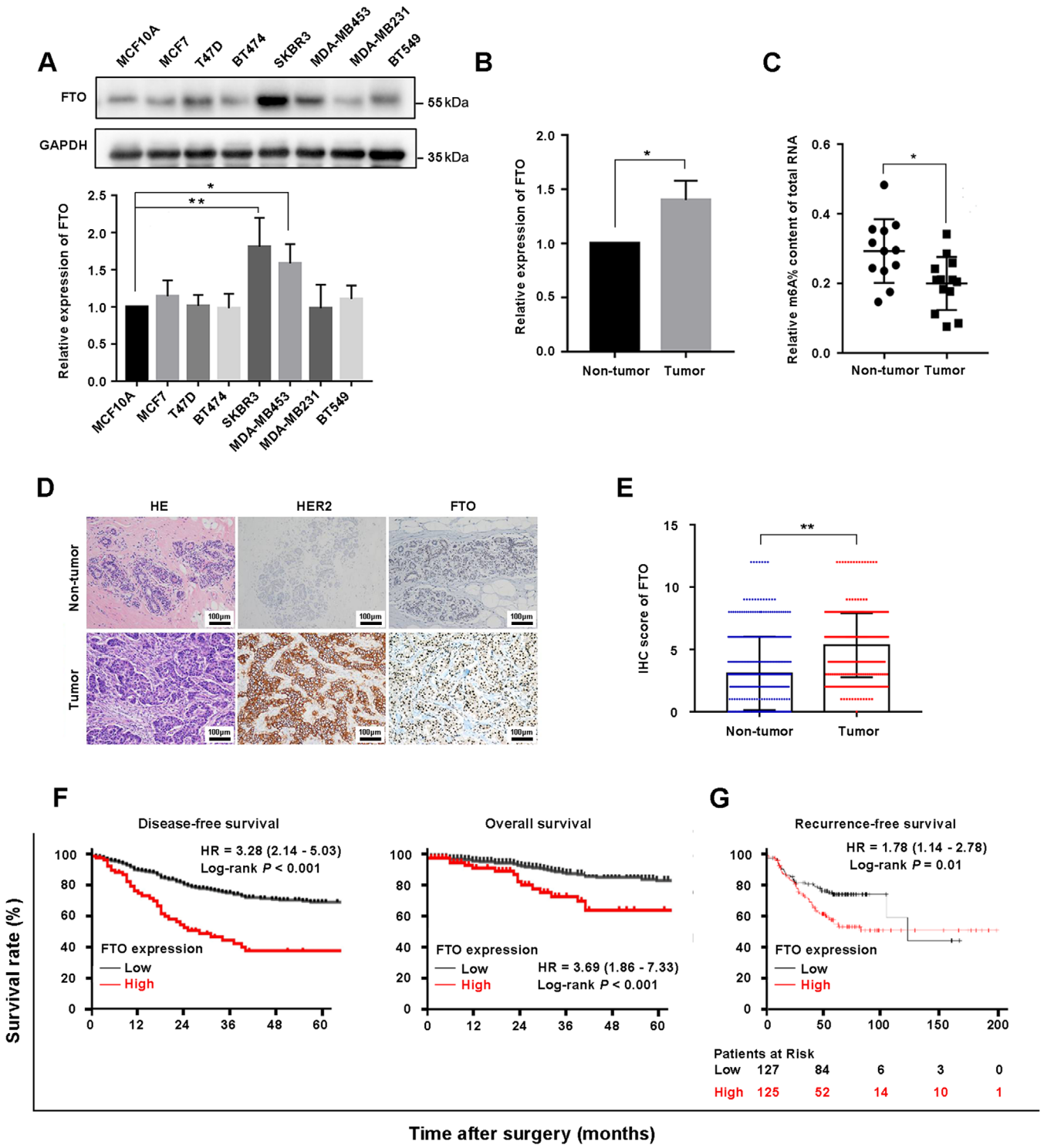

FIGURE 1 FTO is highly expressed in HER2-positive breast cancer tissues and predicts poor prognosis. **A** Relative expression of FTO protein in breast cancer cell lines compared with the immortalized mammary epithelial cell line MCF10A. **B** Relative mRNA level of FTO in HER2-positive breast cancer tissues and paired non-tumor tissues ($n = 12$). C Relative m^6A content of total RNA in paired HER2-positive breast cancer tissues and adjacent non-tumor tissues ($n = 12$). D Representative IHC images of HER2 and FTO expression in tumor and non-tumor tissues. Scale bar: 100 μm. E IHC score of FTO in non-tumor and breast cancer tumor tissues ($n = 408$). F Kaplan-Meier DFS and OS curves stratified by FTO expression in 408 patients with HER2-positive breast cancer. G Kaplan-Meier analysis of RFS based on FTO expression in HER2-positive breast cancer from the online Kaplan-Meier plotter database. * $P < 0.05$, ** $P < 0.01$.

Abbreviations: FTO, fat mass and obesity-associated; HER2, human epidermal growth factor receptor 2; m^6A, N6-methyladenosine; HE, hematoxylin and eosin; IHC, immunohistochemistry; DFS, disease-free survival; OS, overall survival; RFS, recurrence-free survival

TABLE 1 Associations between FTO expression and the clinicopathological characteristics of HER2-positive breast cancer patients

Characteristic	Whole cohort [cases (%)]	FTO expression [cases (%)]		*P* value
		Low	High	
Total	408	308	100	
Age at surgery (years)				0.396
≤50	219 (53.7)	169 (54.9)	50 (50.0)	
> 50	189 (46.3)	139 (45.1)	50 (50.0)	
Tumor size (cm)				< 0.001
≤2.0	127 (31.1)	103 (33.5)	24 (24.0)	
2.1-5.0	242 (59.3)	191 (62.0)	51 (51.0)	
> 5.0	39 (9.6)	14 (4.5)	25 (25.0)	
Nuclear grade*				0.001
II	250 (61.3)	203 (65.9)	47 (47.0)	
III	158 (38.7)	105 (34.1)	53 (53.0)	
LVI				< 0.001
No	356 (87.3)	286 (92.9)	70 (70.0)	
Yes	52 (12.7)	22 (7.1)	30 (30.0)	
LNM				0.002
No	231 (56.6)	188 (61.0)	43 (43.0)	
Yes	177 (43.4)	120 (39.0)	57 (57.0)	
TNM stage#				0.001
I	79 (19.4)	64 (20.8)	15 (15.0)	
II	246 (60.3)	195 (63.3)	51 (51.0)	
III	77 (18.9)	46 (14.9)	31 (31.0)	
IV	6 (1.5)	3 (1.0)	3 (3.0)	

Abbreviations: FTO, fat mass and obesity-associated; HER2, human epidermal growth factor receptor 2; LVI, peritumoral lymphovascular invasion; LNM, lymph node metastasis.

The χ^2 test was used for the comparison between low and high FTO expression groups.

*The nuclear grade was stratified according to the World Health Organization (WHO) classification of breast cancer: grade I, nuclei are similar in size (< 1.5 ×) to benign epithelial cells grade II, nuclei are larger (1.5-2 × the size of benign epithelial cell nuclei) grade III, nuclei are markedly larger in size (> 2 × the size of benign epithelial cell nuclei).

#The TNM stage was classified according to the 8th edition of the American Joint Committee on Cancer (AJCC 8th) staging system.

Prep kit (Illumina, San Diego, CA, USA) according to the manufacturer's instructions. RNAs were single-end sequenced on an Illumina HiSeq™ 2500 Sequencer. All reads were mapped to human genome 19 using BWA tools and annotated by miRBase version 21 (https://www.mirbase.org) using miRDeep2 (https://www.mdc-berlin.de/8551903/en/). RNA-seq data were analyzed using the "edgeR" package in R software (The Free Software Foundation, Boston, MA, USA). Differential expression profiling was filtered with a threshold of |log2 (fold change)| ≥ 1 and P value < 0.05.

2.13 | Bioinformatics analysis

Recurrence-free survival (RFS) curves were generated via the Kaplan-Meier plotter online database (http://kmplot.com/analysis/). By employing miRNA databases (TargetScan, http://www.targetscan.org/vert_72/ miRTarBase, http://mirtarbase.mbc.nctu.edu.tw miRDB, http://www.mirdb.org/ and miRWalk, http://mirwalk.umm.uni heidelberg.de/), we obtained a set of target molecules of miR-181b-3p. The Kyoto Encyclopedia of Genes and Genomes (KEGG) biological pathway enrichment analysis was performed to investigate the involved pathways of miR-181b-3p target molecules by applying KOBAS 3.0 (http://kobas.cbi.pku.edu.cn/). Afterwards, the Venn diagram online tool (http://bioinformatics.psb.ugent.be/webtools/Venn/) was utilized to narrow down the scope into six target molecules. The Oncomine database (http://www.oncomine.org) was used to examine the expression levels of miR-181b-3p target molecules in normal and invasive breast cancer tissues. The binding site of miR-181b-3p to the ARL5B 3′-untranslated region (3′-UTR) was predicted using the miRNA databases mentioned above. A scatter plot of the relative correlation between FTO and ARL5B expression was performed using the R software. The "RTCGA. mRNA" and "dplyr" packages were used

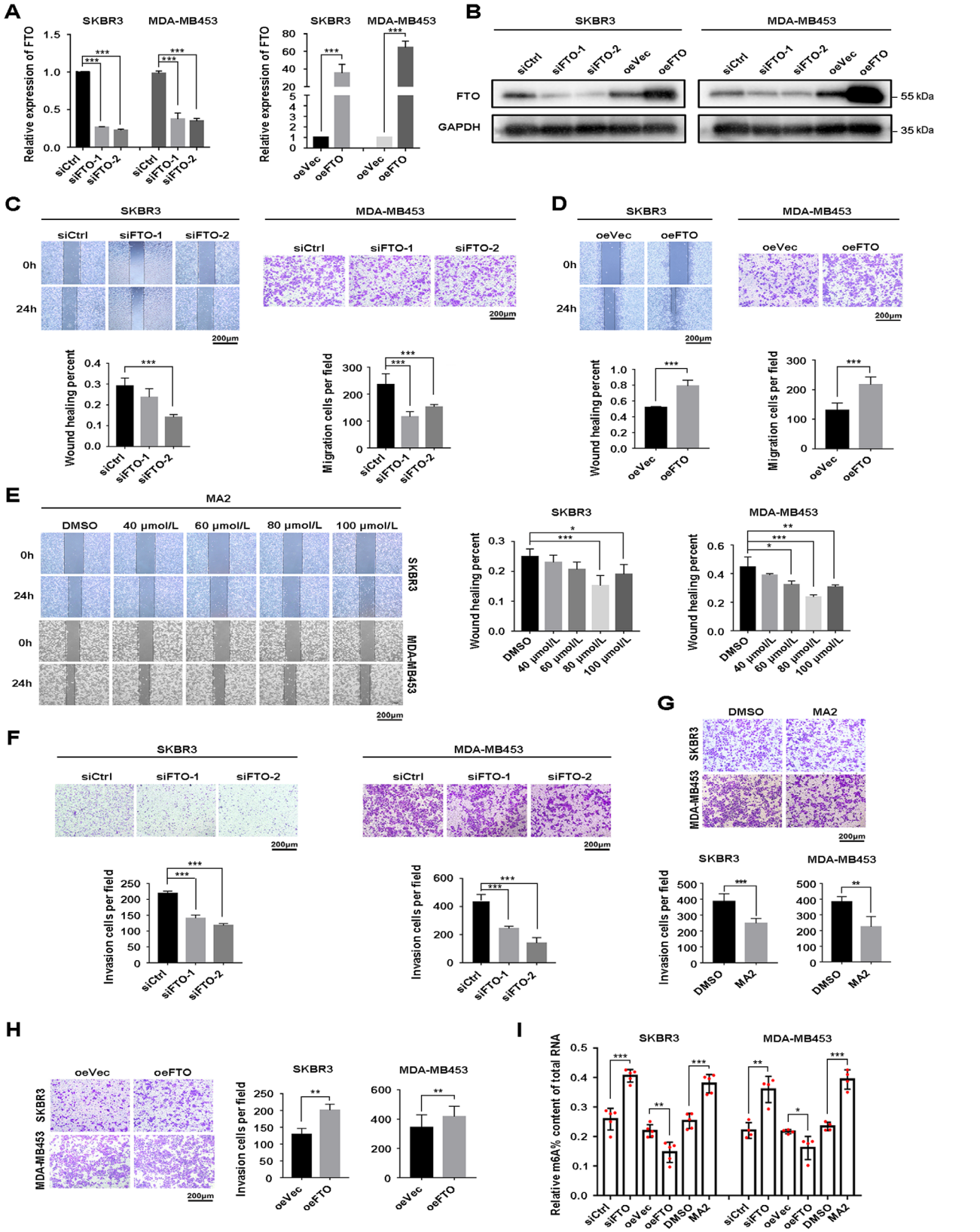

FIGURE 2 FTO enhances the migration and invasion of HER2-positive breast cancer cells. A-B The transfection efficiency of FTO siRNA or overexpression plasmid in SKBR3 and MDA-MB453 cells confirmed by qRT-PCR (A) and Western blotting (B). C-D The detection of cell migration by Wound healing assay in SKBR3 cells and by Transwell migration assay in MDA-MB453 cells. The healing percent and migration cells were measured at 24 h after the transfection of FTO siRNA or overexpression plasmid. E Wound healing assay of SKBR3 and MDA-MB453 cells pretreated with gradient concentrations of MA2 for 48 h. DMSO was used as solvent control. F-G Transwell invasion assay of SKBR3 and MDA-MB453 cells treated with FTO siRNA or MA2 (80 μmol/L). H Transwell invasion assay of SKBR3 and MDA-MB453 cells transfected with

to download and manage data from The Cancer Genome Atlas Program (TCGA, https://portal.gdc.cancer.gov/). The "ggpubr" package was used to draw the scatter plot.

2.14 | Luciferase reporter assay

DNA fragments containing the wild-type or mutant 3′-UTR of ARL5B were separately inserted into the pmirGLO vector (Public Protein/Plasmid Library, Nanjing, Jiangsu, China). HEK-293T cells were co-transfected with plasmids containing ARL5B 3′-UTR wild-type or mutant fragments and miR-181b-3p mimics or miRNC using Lipofectamine 3000. After 48 h of co-transfection, luciferase reporter assays were performed using the Dual Luciferase Reporter Assay System (Promega Corporation, Madison, WI, USA). The ratio of luminescence signals from firefly luciferase to those from Renilla luciferase was calculated to assess the binding of miR-181b-3p and ARL5B.

2.15 | Statistical analyses

Statistical analyses were performed using IBM SPSS Statistics version 22.0 (SPSS Inc., Chicago, IL, USA) and GraphPad Prism 7.0 (GraphPad Software Inc., La Jolla, CA, USA). Data are presented as the mean ± standard deviation. Significant differences were calculated by two-tailed Student's *t*-test or one-way analysis of variance (one-way ANOVA). The Kaplan-Meier method and log-rank test were applied to determine disease-free survival (DFS) and overall survival (OS), which were defined as the intervals from surgery to the occurrence of disease or death of any cause. The chi-squared test was utilized to detect the association between FTO expression and clinicopathological factors. Experiments were repeated independently at least three times. P value < 0.05 was considered statistically significant.

3 | RESULTS

3.1 | The expression of FTO and its clinical significance in HER2-positive breast cancer

We first examined the expression of FTO in breast cancer cells compared with MCF10A cells, and FTO was observed to be highly expressed exclusively in the HER2-positive cell lines SKBR3 and MDA-MB453 (Figure 1A). Moreover, compared with non-tumor tissues, HER2-positive breast cancer tissues showed increased mRNA levels of FTO (Figure 1B). Due to the m^{6}A demethylase function of FTO, we found that m^{6}A was irregularly down-regulated in HER2-positive breast cancer tissues (Figure 1C). In addition, IHC staining was conducted and demonstrated that FTO was expressed at higher levels in HER2-positive breast cancer tissues than in non-tumor tissues (Figure 1D-1E).

The clinical significance of aberrantly expressed FTO in HER2-positive breast cancer was analyzed, and the results showed that FTO expression was significantly associated with tumor size ($P < 0.001$), nuclear grade ($P = 0.001$), peritumoral lymphovascular invasion ($P < 0.001$), lymph node metastasis ($P = 0.002$), and TNM stage ($P = 0.001$) (Table 1). Kaplan-Meier DFS and OS curves suggested that high expression of FTO predicted poor prognosis (Figure 1F). Similarly, RFS of HER2-positive breast cancer cases from the Kaplan-Meier plotter online database implied that high levels of FTO were related to increased tumor recurrence risk (Figure 1G).

3.2 | The pro-tumor role of FTO in HER2-positive breast cancer cells

Knockdown and overexpression of FTO were carried out in SKBR3 and MDA-MB453 cells, and corresponding changes in the expression of FTO were confirmed in both cell lines (Figure 2A-2B). By wound healing assay in SKBR3 cells and Transwell migration assay in MDA-MB453 cells, cell migration was decreased upon FTO knockdown but accelerated upon FTO overexpression (Figure 2C-2D). A wound healing assay in FTO-silenced MDA-MB453 cells also showed inhibited cell migration (Supplementary Figure S1A). In addition, we observed inhibition of cell migration with MA2 treatment, and the inhibition effect was maximal at 80 μmol/L (Figure 2E). Correspondingly, FTO inhibition by siRNA or MA2 was found to impair cell invasion (Figure 2F and 2G), while the results were reversed when FTO was overexpressed (Figure 2H). However, cell proliferation was not distinctly changed after FTO alteration (Supplementary Figure S1B). Furthermore, m^{6}A quantification assay showed that inhibition of FTO increased m^{6}A levels, while FTO overexpression decreased m^{6}A abundance (Figure 2I).

FTO plasmid. Experiments were terminated after seeding for 24 h. I Relative m^{6}A content of total RNA after FTO knockdown, overexpression, or FTO inhibitor MA2 treatment. Scale bar: 200 μm. * $P < 0.05$, ** $P < 0.01$, *** $P < 0.001$.

Abbreviations: siCtrl, negative control of siRNA; siFTO, FTO siRNA; eVec, empty plasmid vector; oeFTO, FTO clone plasmid; qRT-PCR, quantitative reverse transcription-PCR; MA2, the ethyl ester form of meclofenamic acid other abbreviations as in Figure 1

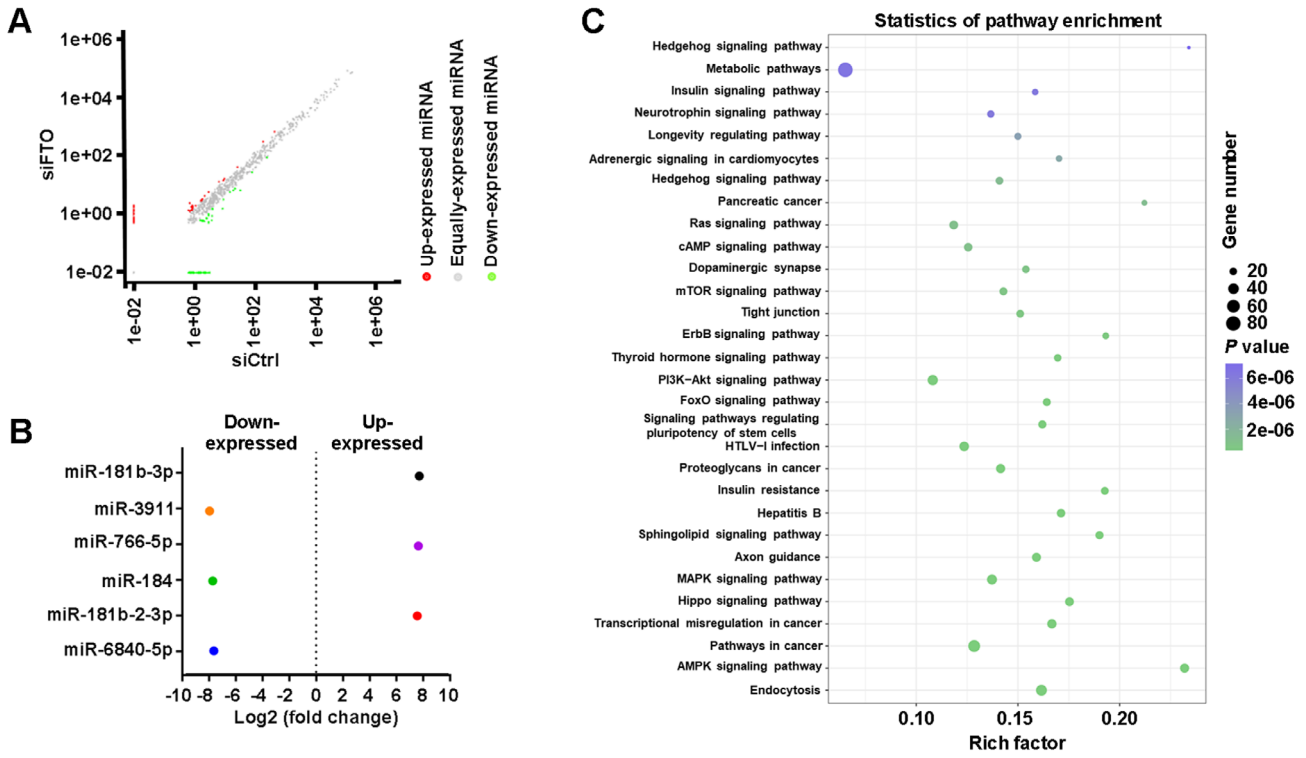

FIGURE 3 Identification of miRNAs and pathways related to FTO alteration by RNA-sequencing. **A** The discrepancy in miRNA expression in FTO-silenced SKBR3 cells compared with negative control cells. **B** The top six up-regulated or down-regulated miRNAs. **C** The pathway enrichment analysis of miRNA target genes in FTO knockdown SKBR3 cells compared with negative control cells.
Abbreviations: miRNAs, microRNAs; FTO, fat mass and obesity-associated

3.3 | Identification of FTO downstream targets by RNA-seq

To explore potential targets of FTO, we performed RNA-seq on FTO-knockdown SKBR3 cells. RNA-seq analysis revealed that 19 miRNAs were significantly down-regulated, while 10 miRNAs were significantly up-regulated (Figure 3A) the top six up-regulated or down-regulated miRNAs are listed in Figure 3B. The KEGG pathway enrichment analysis of miRNA target genes showed that metabolic pathways were intensely clustered, followed by pathways in cancer and endocytosis (Figure 3C).

We selected miR-181b-3p, the miRNA with the greatest change, to test the relationship between FTO and miRNAs in HER2-positive breast cancer. qRT-PCR analysis confirmed that FTO inhibition using siRNA or MA2 resulted in significantly increased levels of miR-181b-3p, while FTO overexpression reduced miR-181b-3p expression (Figure 4). miR-181b-3p depletion mimicked the FTO-mediated promotion of breast cancer cell migration and invasion (Figure 5A-5B), whereas miR-181b-3p overexpression yielded opposite results (Figure 5C-5D). Dysregulation of miR-181b-3p also significantly reversed the inhibitory effect of MA2 (Figure 5E and 5F).

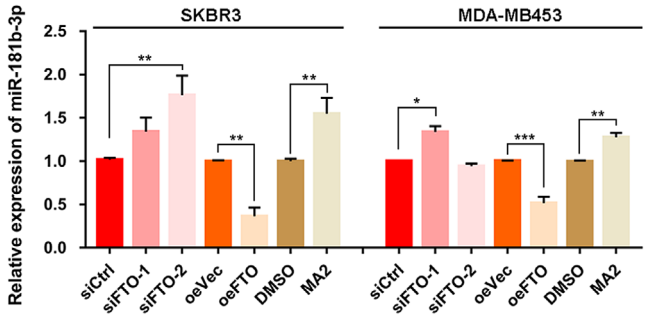

FIGURE 4 The regulation of FTO on miR-181b-3p expression. The relative level of miR-181b-3p in SKBR3 and MDA-MB453 cells treated with FTO siRNA, FTO overexpression plasmid, or MA2 (80 μmol/L). *$P < 0.05$, **$P < 0.01$, ***$P < 0.001$. Abbreviations are the same as in Figure 2

3.4 | Potential of ARL5B as a novel target of miR-181b-3p and its regulation by FTO

Based on the prediction of miR-181b-3p targets by bioinformatics analysis, six candidate molecules were identified (Figure 6A): ARL5B, Ras-related protein Rap-2c (RAP2C), clathrin light chain A (CLTA), protein-L-isoaspartate (D-aspartate) O-methyltransferase domain containing 1

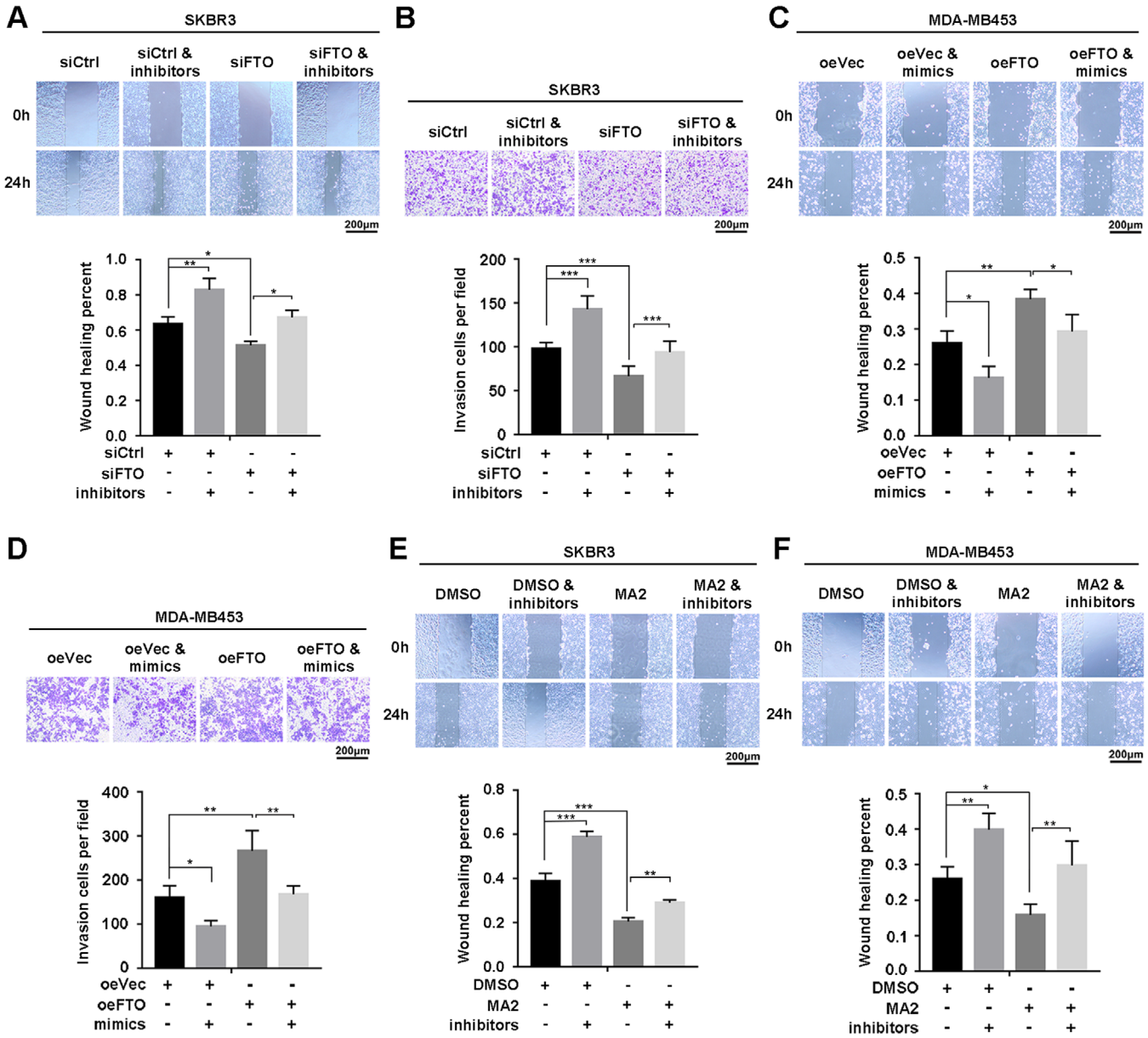

FIGURE 5 miR-181b-3p inhibits the pro-tumor effects of FTO in HER2-positive breast cancer cells. A-B Wound healing assay and Transwell invasion assay in control or FTO-depleted SKBR3 cells with or without the presence of miR-181b-3p inhibitors. C-D Wound healing assay and Transwell invasion assay in control or FTO-overexpressing MDA-MB453 cells with or without the presence of miR181b-3p mimics. E-F Wound healing assay in DMSO or MA2 (80 μmol/L) treated SKBR3 and MDA-MB453 cells with or without the presence of miR-181b-3p inhibitors. * $P < 0.05$, ** $P < 0.01$, *** $P < 0.001$. Scale bar: 200 μm. Abbreviations are the same as in Figure 2

(PCMTD1), ribosomal modification protein rimK like family member B (RIMKLB), and sosondowah ankyrin repeat domain family member B (SOWAHB), of which ARL5B and RIMKLB mRNA were found to be significantly down-regulated in FTO-silenced cells according to RNA-seq analysis (data not shown). Further confirmation by qRT-PCR demonstrated that the expression of ARL5B and PCMTD1 was significantly inhibited with transfection of miR-181b-3p mimics (Figure 6B and 6C), while ARL5B, RAP2C, PCMTD1, and RIMKLB were elevated with transfection of miR-181b-3p inhibitors (Figure 6D and 6E). Similarly, the expression of all candidate molecules except SOWAHB was decreased upon FTO knockdown (Figure 6F and 6G), whereas only ARL5B, CLTA, and RIMKLB showed up-regulation upon FTO overexpression (Figure 6H and 6I), while ARL5B, RAP2C, CLTA, and RIMKLB were substantially reduced upon MA2 treatment (Figure 6J and 6K). The expression of five candidate molecules in breast cancer tissues was also investigated (no SOWAHB data online), of which only ARL5B and RAP2C were

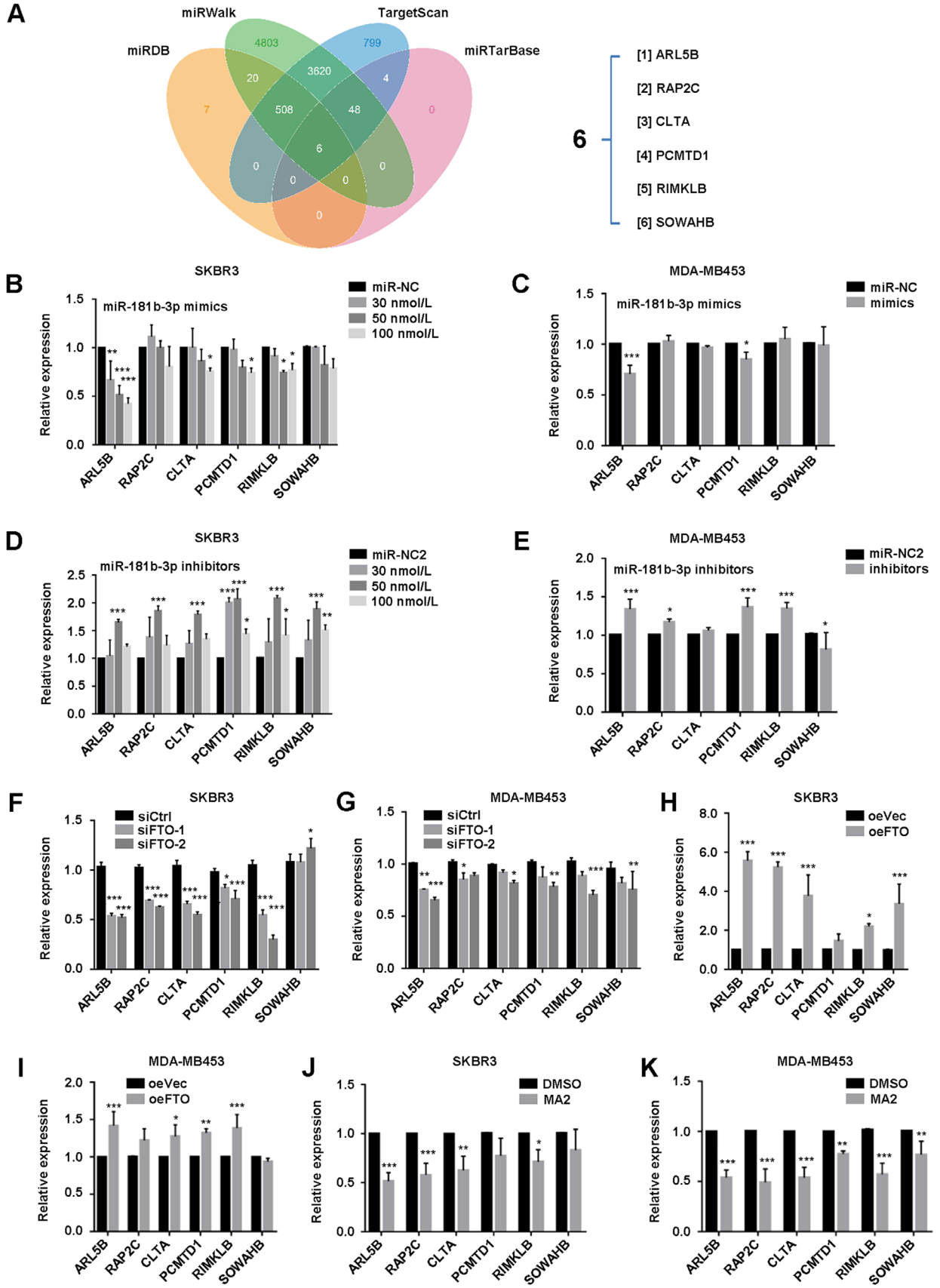

FIGURE 6 FTO positively mediates the expression of miR-181b-3p downstream targets. A The Venn diagram refined six potential targets of miR-181b-3p: ARL5B, RAP2C, CLTA, PCMTD1, RIMKLB, and SOWAHB. B-C qRT-PCR analysis of the expression of the six candidate molecules in SKBR3 and MDA-MB453 cells with the transfection of miR-181b-3p mimics. D-E qRT-PCR analysis of the expression of the six candidate

aberrantly up-regulated in invasive breast tumor (Supplementary Figure S2). Kaplan-Meier analysis in breast cancer patients suggested that high levels of ARL5B, RAP2C, and CLTA and low levels of PCMTD1 and RIMKLB were significantly associated with short RFS (Supplementary Figure S3). Overall, ARL5B was identified as the downstream target of interest.

We next focused on the relationship between ARL5B and FTO or miR-181b-3p. The results showed that FTO reinforced ARL5B expression, while miR-181b-3p inhibited ARL5B expression (Figure 7A-7C). Correlation analysis revealed that the expression levels of FTO and ARL5B were positively correlated (Figure 7D), and the dual luciferase reporter assay confirmed that miR-181b-3p bound directly to the ARL5B 3′-UTR (Figure 7E-7F). Furthermore, by transfecting siARL5B into FTO-overexpressing cells or ARL5B clone plasmid into FTO-silenced cells, ARL5B was verified to be able to drive the migration and invasion effects induced by FTO (Figure 8A-8D). Overexpressing ARL5B after MA2 treatment also rescued the inhibitory effect of MA2 (Figure 8E and 8F). Additionally, we knocked down or enhanced the expression of ARL5B in SKBR3 and MDA-MB453 cells. Based on satisfactory transfection efficiency (Figure 9A-9D), ARL5B silencing markedly reduced tumor cell migration and invasion, while forced expression of ARL5B yielded the opposite effects (Figure 9E-9H). In summary, these data indicate that FTO could accelerate the migration and invasion of HER2-positive breast cancer cells via the FTO/miR-181b-3p/ARL5B signaling pathway (Figure 10).

4 | DISCUSSION

The contribution of FTO to the risk of various cancers shown in epidemiological studies [12], along with its aberrant expression in breast cancer, indicates the possible involvement of FTO in mediating the pathological development of breast cancer. In the present study, we discovered that FTO was highly expressed in HER2-positive breast cancer cells and tissues. Statistical analysis of clinical characteristics and survival of HER2-positive breast cancer patients suggested that a high level of FTO was significantly associated with poor clinical outcomes. Mechanistically, in SKBR3 and MDA-MB453 cells, FTO accelerated cell migration and invasion by targeting ARL5B via miR-181b-3p down-regulation. Furthermore, ARL5B was shown to promote breast tumor cell migration and invasion. Together, these findings reveal the prognostic value of FTO and provide novel insight into the role of the FTO/miR-181b-3p/ARL5B axis in the pathogenesis of breast cancer.

Tan et al. [27] discovered that FTO expression was significantly associated with clinicopathological characteristics of HER2-positive breast cancer patients, which aligns with our current results. In addition to our findings in SKBR3 and MDA-MB453 cells, Niu et al. [15] proposed that FTO induced breast cancer cell proliferation and metastasis by epigenetically demethylating the 3′-UTR of the pro-apoptosis factor BCL2 interacting protein 3 (BNIP3) in MCF7 and MDA-MB231 cells. This observation implied the intricate involvement of FTO in different breast cancer molecular subtypes, which is worthy of further exploration. Su et al. [28] discovered that R-2-hydroxyglutarate exerted antitumor activity by targeting the FTO/m^{6}A/MYC/CEBPA signaling pathway, leading to suppressed proliferation or survival of leukemia and glioma cells expressing high levels of FTO. Li et al. [13] showed that FTO reduced the transcription of ankyrin repeat and SOCS box containing 2 (ASB2) and retinoic acid receptor alpha (RARA) by serving as an m^{6}A demethylase, promoting proliferation and inhibiting apoptosis in acute myeloid leukemia. Similarly, treatment with the FTO inhibitor MA2 and subsequent m^{6}A detection in the present study suggested that FTO exerted a pro-tumor function by removing the m^{6}A modification. Moreover, based on the study by Berulava et al. [23] searching for the possible consensus sequence motifs for m^{6}A modification in m^{6}A immunoprecipitated miRNAs, we succeeded in mapping the miR-181b-3p sequence to all the most discriminating motifs, and the mapped sequence was enriched in the center section. The miR-181b-3p sequence also contains the "RRACH" motif which has been identified as a highly conserved common sequence for m^{6}A modification of mRNA and long non-coding RNA [29, 30]. These results may imply the direct interaction between FTO and miR-181b-3p. However, MeRIP-seq should be applied to fully clarify the specific m^{6}A modification site of miR-181b-3p that is modified by FTO. Based on the crucial role of FTO in metabolism, although no difference in cell viability was detected in our research, we do not exclude the possibility that FTO is involved in breast cancer cell

molecules in SKBR3 and MDA-MB453 cells with the transfection of miR-181b-3p inhibitors. F-K The mRNA levels of candidate molecules in SKBR3 and MDA-MB453 cells treated with FTO siRNA (F-G), FTO plasmid (H-I), or MA2 (80 μmol/L, J-K). * $P < 0.05$, ** $P < 0.01$, *** $P < 0.001$. Abbreviations: miR-NC, negative control of miR-181b-3p mimics; miR-NC2, negative control of miR-181b-3p inhibitors; ARL5B, ADP ribosylation factor like GTPase 5B; RAP2C, Ras-related protein Rap-2c; CLTA, clathrin light chain A; PCMTD1, protein-L-isoaspartate (D-aspartate) O-methyltransferase domain containing 1; RIMKLB, ribosomal modification protein rimK like family member B; SOWAHB, sosondowah ankyrin repeat domain family member B; other abbreviations as in Figure 2

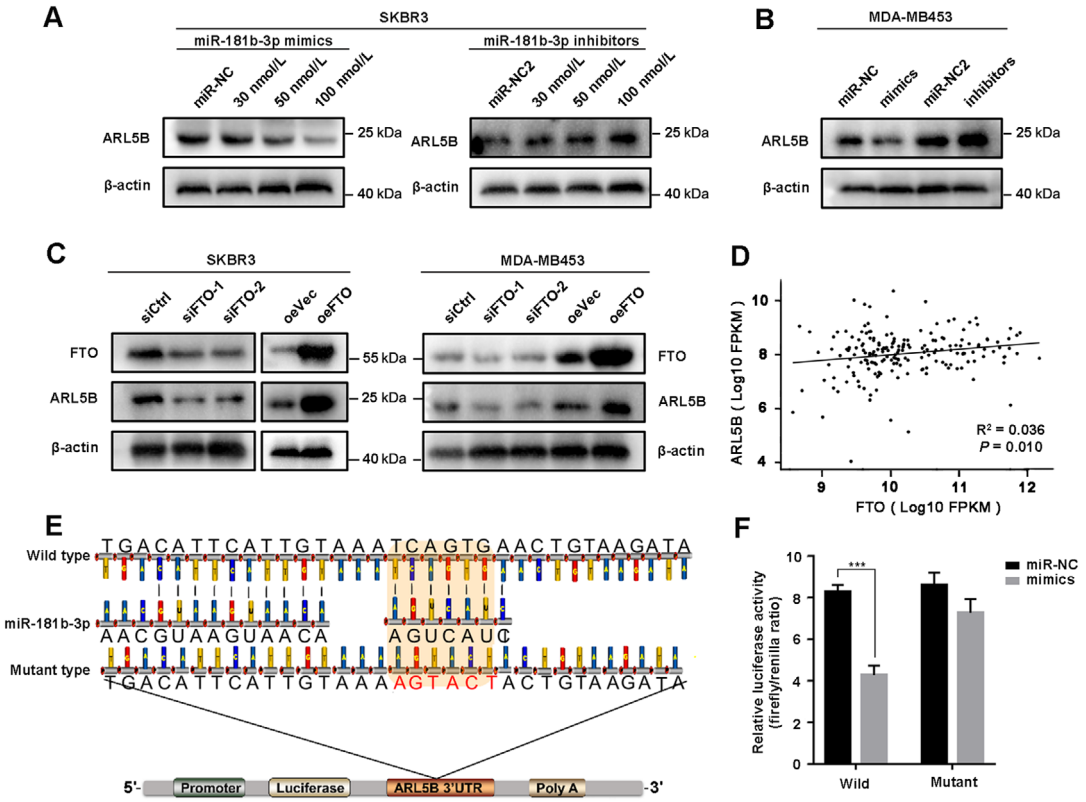

FIGURE 7 ARL5B is the target of miR-181b-3p and positively regulated by FTO. A-B The protein level of ARL5B in SKBR3 and MDA-MB453 cells with transfection of miR-181b-3p mimics or inhibitors. C The protein level of ARL5B in FTO-silenced or -overexpressing SKBR3 and MDA-MB453 cells. D The scatter plot between the expression of FTO and ARL5B in HER2-positive breast cancer (data from TCGA, $R^2 = 0.036$, $P = 0.010$). E Schematic illustration of miR-181b-3p and ARL5B 3′ UTR-binding sites accompanied with wild-type and mutant-type sequences of ARL5B 3′-UTR reporter plasmid. The shaded area denoted the complementary bases and corresponding mutated nucleobases. F Luciferase reporter gene assay in HEK-293T cells following co-transfection of ARL5B wild type or mutant type and miR-181b-3p mimics or miR-NC, respectively (*** $P < 0.001$).

Abbreviations: TCGA, The Cancer Genome Atlas Program; FPKM: Fragments Per Kilobase Million; 3′-UTR, 3′-untranslated region; other abbreviations as in Figure 6

proliferation and apoptosis. Further studies are urged to fully unveil the comprehensive role of FTO in breast cancer.

In the present study, we confirmed that FTO could reduce the expression of miR-181b-3p, which inhibited the pro-tumor effects of FTO. The miR-181 family has been clarified to be critical for cell cycle progression and differentiation [31]. miR-181b-3p was found to promote tumor epithelial-mesenchymal transition by snail stabilization in MCF7, BT549, and MDA-MB231 cells [32], whereas miR-181b inhibited the migration of MCF7 and MDA-MB231 cells [33]. In the present study, miR-181b-3p inhibited the migration and invasion of HER2-positive breast cancer cells by targeting ARL5B. The fact that miR-181b-3p could exhibit diverse biological roles in different cellular contexts indicates that miRNAs are under delicate and intricate control. The illumination of its regulatory mechanism will be helpful to clarify the clinical significance of miR-181b-3p in different circumstances [34].

To date, ARL5B has been recognized as a member of the ADP ribosylation factor-like (ARL) family belonging to the RAS superfamily [35]. In addition to being conserved, ARL5B is the only small G protein present on mature lysosomes [36, 37]. Previous studies have demonstrated that ARL5B overexpression facilitated lysosome motility, resulting in lysosome dispersion and accumulation at the cell periphery [38, 39]. Lysosomes move toward the cell periphery along microtubules in a kinesin-1-SKIP-ARL5B-dependent manner, which is essential for focal adhesion turnover and cathepsin exocytosis in the process of cell migration [40, 41]. The guided outward movement of lysosomes is considered to be a critical determinant of lysosomal function [42, 43]. The present research discovered that ARL5B enhanced breast tumor cell migration and

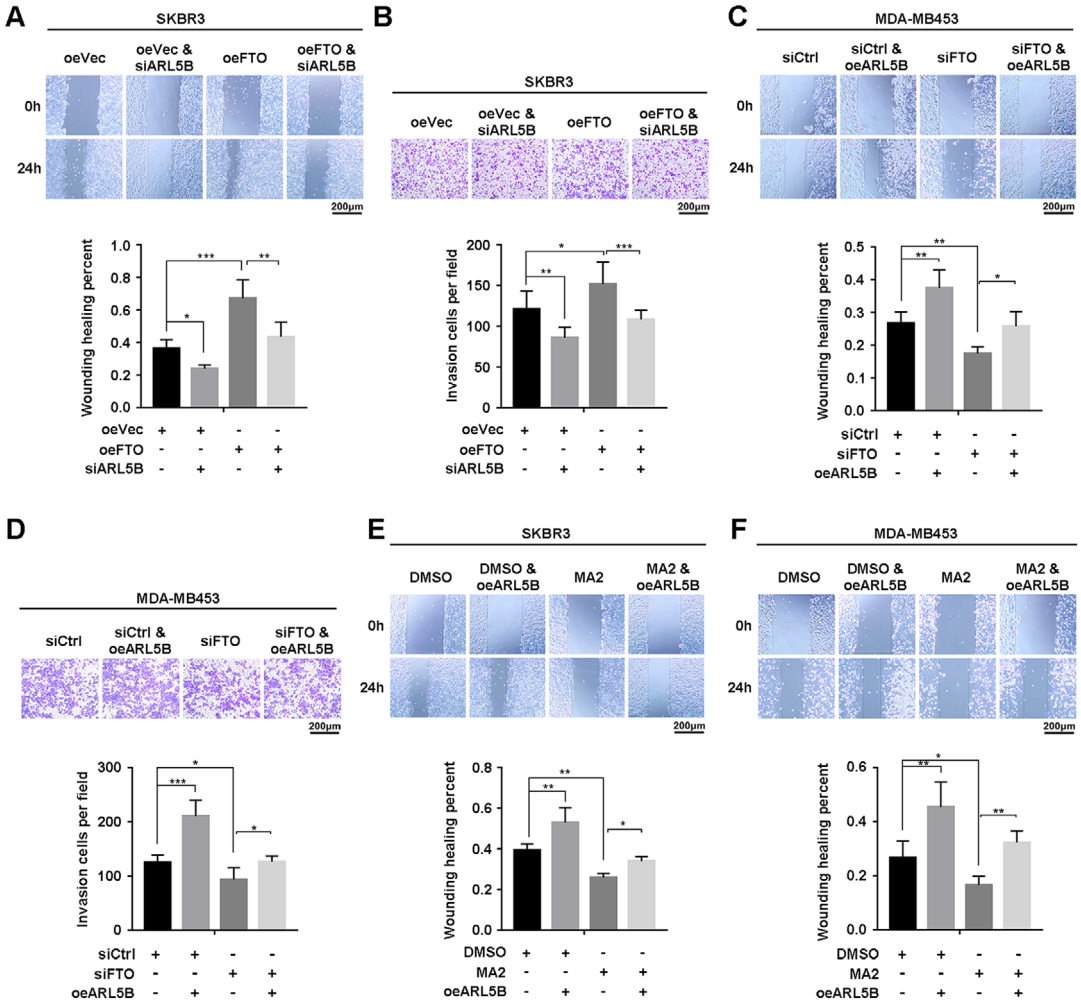

FIGURE 8 ARL5B can mediate the migration and invasion of breast cancer cells induced by FTO. A-B Wound healing assay and Transwell invasion assay in control or FTO-overexpressing SKBR3 cells with or without the presence of siARL5B. C-D Wound healing assay and Transwell invasion assay in control or FTO depleted SKBR3 and MDA-MB453 cells with or without ARL5B forced expression. E-F Wound healing assay in DMSO or MA2 (80 μmol/L) treated SKBR3 and MDA-MB453 cells with or without the presence of ARL5B overexpression. * $P < 0.05$, ** $P < 0.01$, *** $P < 0.001$. Scale bar: 200 μm.

Abbreviations: ARL5B, ADP ribosylation factor like GTPase 5B; siARL5B, ARL5B siRNA; oeARL5B, ARL5B clone plasmid; other abbreviations as in Figure 2

invasion, implying an oncogenic role in breast cancer. Moreover, in SKBR3 and MDA-MB453 cells, Rafn et al. [44] detected that decreased lysosomal outward trafficking resulted in inhibited cancer cell invasion. Additionally, ARL5B silencing reduced lysosome dispersion and subsequently decreased cell invasion in prostate cancer [45]. Taken together, these results suggest that ARL5B may enhance the migration and invasion of breast cancer cells by accelerating the redistribution of lysosomes to the cell periphery.

In our present study, we failed to pinpoint the exact m^{6}A modification site in miR-181b-3p by MeRIP-seq. In addition, the explicit mechanism of how ARL5B drives cell invasion and migration has not been clearly explored. Moreover, an *in vivo* study is essential to confirm the cancer-promoting role of FTO and ARL5B at the integral level. Further studies are needed to fully unfold the clinical value of FTO, miR-181b-3p, and ARL5B in breast cancer.

5 | CONCLUSIONS

In the current study, we provide clinical and *in vitro* evidence that FTO, which is highly expressed in HER2-positive breast cancer, could promote cell migration and

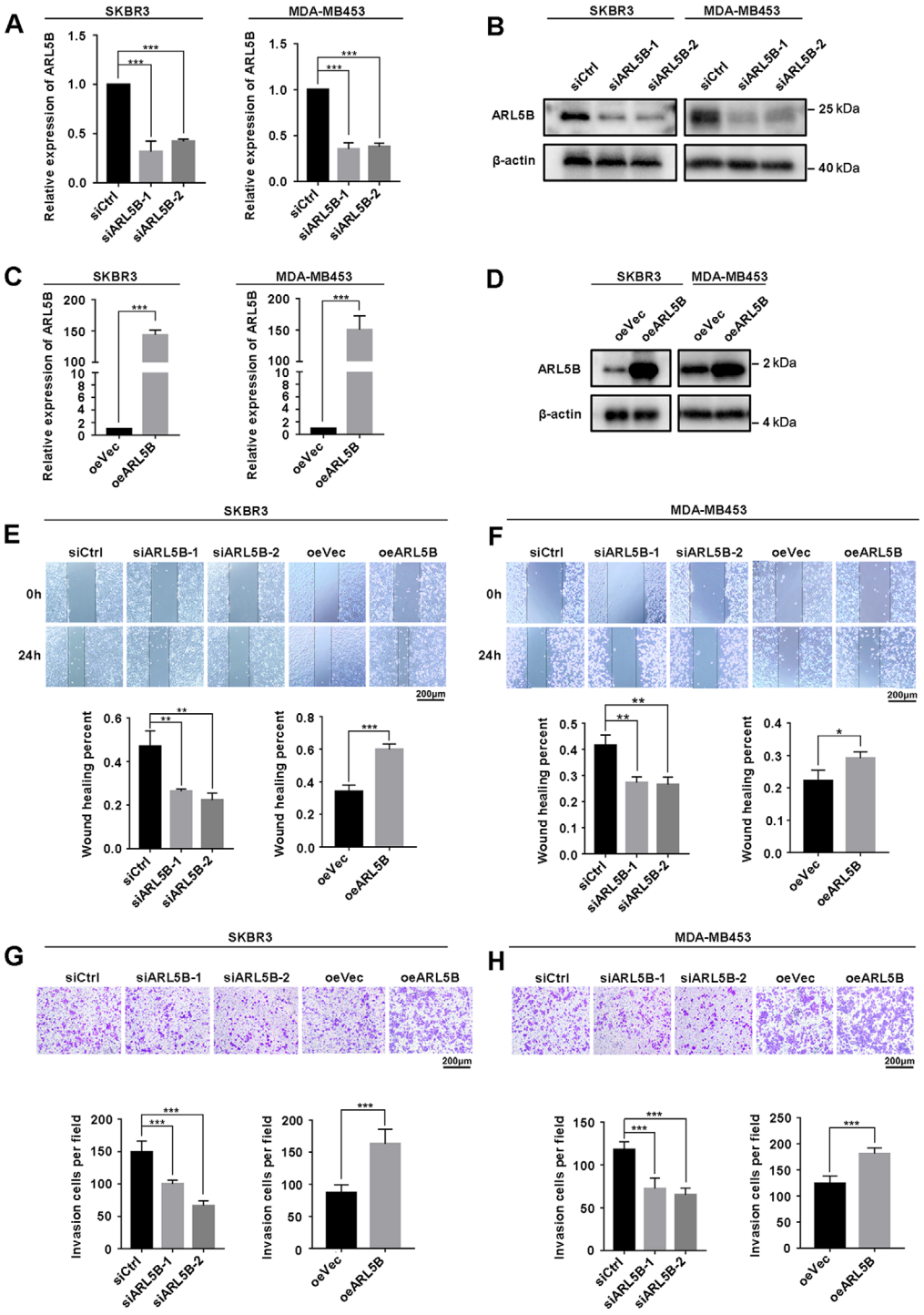

FIGURE 9 ARL5B plays an oncogenic role in HER2-positive breast cancer cells. A-D The transfection efficiency of ARL5B siRNA and overexpression plasmid in SKBR3 and MDA-MB453 cells by qRT-PCR and Western blotting. E-F Wound healing assay of SKBR3 and MDA-MB453 cells with ARL5B depletion or overexpression. Experiments were terminated after scratch for 24 h. G-H Transwell invasion assay in ARL5B-silenced or -overexpressing SKBR3 and MDA-MB453 cells. * $P < 0.05$, ** $P < 0.01$, *** $P < 0.001$. Scale bar: 200 μm. Abbreviations are the same as in Figure 8

invasion through the FTO/miR-181b-3p/ARL5B signaling pathway. Our work highlights the functional involvement of FTO in tumor pathogenesis and uncovers the cancer-promoting role of ARL5B, indicating the potential prognostic value for breast cancer. Future work is urged to shed light on the clinical significance of miR-181b-3p and ARL5B in breast cancer and to search for possible predictive factors.

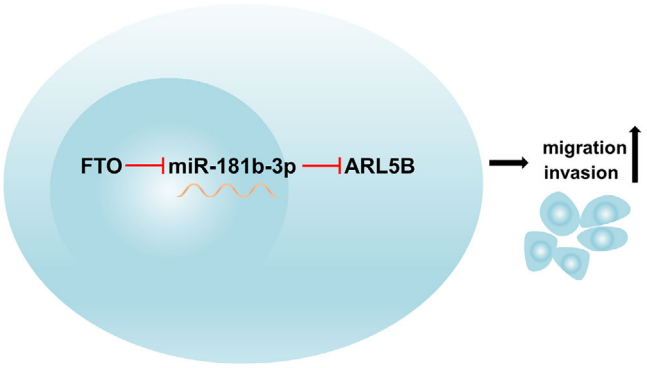

FIGURE 10 The schematic model of the role and underlying mechanism of FTO in breast cancer.
Abbreviations: FTO, fat mass and obesity-associated; ARL5B, ADP ribosylation factor like GTPase 5B

ACKNOWLEDGEMENTS

The authors thank Prof. Caiguang Yang and Dr. Ze Dong (Shanghai Institute of Materia Medical, Chinese Academy of Sciences) for donating the drug reagent MA2. Thanks to Jing Yang (Zhongshan School of Medicine, Sun Yat-sen University) for generous help in technical support.

AUTHORS' CONTRIBUTIONS

THW and PS designed and funded the study. YYX, SY, and NZ conducted the experiments and analyzed the data. HTL and YC performed bioinformatic data analyses. LW provided experimental material support. SHZ and KWZ provided supervision and suggestions for the implementation of the study. YYX and SY drafted the manuscript. THW, PS, and KWZ guided and reviewed the manuscript. All authors read and approved the final manuscript.

ETHICS APPROVAL AND CONSENT TO PARTICIPATE

This study was approved by the Institutional Ethical Boards of Sun Yat-sen University Cancer Center. Written informed consent was obtained from all patients.

CONSENT FOR PUBLICATION

Not applicable.

AVAILABILITY OF DATA AND MATERIALS

Not applicable.Sad

COMPETING INTERESTS

The authors declare that they have no competing interests.

ORCID

Tinghuai Wang https://orcid.org/0000-0001-6681-8188

REFERENCES

1. Siegel RL, Miller KD, Jemal A. Cancer statistics, 2019. CA Cancer J Clin. 2019;69(1):7-34.
2. Pan H, Gray R, Braybrooke J, Davies C, Taylor C, McGale P, et al. 20-Year Risks of Breast-Cancer Recurrence after Stopping Endocrine Therapy at 5 Years. N Engl J Med. 2017;377(19):1836-46.
3. Lambert AW, Pattabiraman DR, Weinberg RA. Emerging Biological Principles of Metastasis. Cell. 2017;168(4):670-91.
4. Ci Y, Qiao J, Han M. Molecular Mechanisms and Metabolomics of Natural Polyphenols Interfering with Breast Cancer Metastasis. Molecules. 2016;21(12).
5. Chua BA, Van Der Werf I, Jamieson C, Signer RAJ. Post-Transcriptional Regulation of Homeostatic, Stressed, and Malignant Stem Cells. Cell Stem Cell. 2020;26(2):138-59.
6. Obeng EA, Stewart C, Abdel-Wahab O. Altered RNA Processing in Cancer Pathogenesis and Therapy. Cancer discovery. 2019;9(11):1493-510.
7. Shi H, Wei J, He C. Where, When, and How: Context-Dependent Functions of RNA Methylation Writers, Readers, and Erasers. Mol Cell. 2019;74(4):640-50.
8. Frye M, Harada BT, Behm M, He C. RNA modifications modulate gene expression during development. Science. 2018;361(6409):1346-9.
9. Zhao BS, Roundtree IA, He C. Post-transcriptional gene regulation by mRNA modifications. Nat Rev Mol Cell Biol. 2017;18(1):31-42.
10. Loos RJ, Yeo GS. The bigger picture of FTO: the first GWAS-identified obesity gene. Nat Rev Endocrinol. 2014;10(1):51-61.
11. Jia G, Fu Y, Zhao X, Dai Q, Zheng G, Yang Y, et al. N6-methyladenosine in nuclear RNA is a major substrate of the obesity-associated FTO. Nat Chem Biol. 2011;7(12):885-7.
12. Chen J, Du B. Novel positioning from obesity to cancer: FTO, an m(6)A RNA demethylase, regulates tumour progression. J Cancer Res Clin Oncol. 2019;145(1):19-29.
13. Li Z, Weng H, Su R, Weng X, Zuo Z, Li C, et al. FTO Plays an Oncogenic Role in Acute Myeloid Leukemia as a N(6)-Methyladenosine RNA Demethylase. Cancer Cell. 2017;31(1):127-41.
14. Cui Q, Shi H, Ye P, Li L, Qu Q, Sun G, et al. m(6)A RNA Methylation Regulates the Self-Renewal and Tumorigenesis of Glioblastoma Stem Cells. Cell Rep. 2017;18(11):2622-34.
15. Niu Y, Lin Z, Wan A, Chen H, Liang H, Sun L, et al. RNA N6-methyladenosine demethylase FTO promotes breast tumor progression through inhibiting BNIP3. Mol Cancer. 2019;18(1):46.
16. Kaklamani V, Yi N, Sadim M, Siziopikou K, Zhang K, Xu Y, et al. The role of the fat mass and obesity associated gene (FTO) in breast cancer risk. BMC Med Genet. 2011;12:52-.
17. Yang ZQ, Liu G, Bollig-Fischer A, Giroux CN, Ethier SP. Transforming properties of 8p11-12 amplified genes in human breast cancer. Cancer Res. 2010;70(21):8487-97.
18. Ragvin A, Moro E, Fredman D, Navratilova P, Drivenes Ø, Engström PG, et al. Long-range gene regulation links genomic type 2 diabetes and obesity risk regions to HHEX, SOX4, and IRX3. Proc Natl Acad Sci U S A. 2010;107(2):775-80.
19. Gebert LFR, MacRae IJ. Regulation of microRNA function in animals. Nat Rev Mol Cell Biol. 2019;20(1):21-37.

20. Fazi F, Fatica A. Interplay Between N (6)-Methyladenosine (m(6)A) and Non-coding RNAs in Cell Development and Cancer. Front Cell Dev Biol. 2019;7:116.
21. Ma JZ, Yang F, Zhou CC, Liu F, Yuan JH, Wang F, et al. METTL14 suppresses the metastatic potential of hepatocellular carcinoma by modulating N(6) -methyladenosine-dependent primary MicroRNA processing. Hepatology. 2017;65(2):529-43.
22. Han J, Wang JZ, Yang X, Yu H, Zhou R, Lu HC, et al. METTL3 promote tumor proliferation of bladder cancer by accelerating pri-miR221/222 maturation in m6A-dependent manner. Mol Cancer. 2019;18(1):110.
23. Berulava T, Rahmann S, Rademacher K, Klein-Hitpass L, Horsthemke B. N6-adenosine methylation in MiRNAs. PloS one. 2015;10(2):e0118438.
24. Ye S, Xu Y, Li J, Zheng S, Sun P, Wang T. Prognostic role of GPER/Ezrin in triple negative breast cancer is associated with menopausal status. Endocr Connect. 2019;8(6):661-71.
25. Huang Y, Yan J, Li Q, Li J, Gong S, Zhou H, et al. Meclofenamic acid selectively inhibits FTO demethylation of m6A over ALKBH5. Nucleic Acids Res. 2015;43(1):373-84.
26. Zhou K, Sun P, Zhang Y, You X, Li P, Wang T. Estrogen stimulated migration and invasion of estrogen receptor-negative breast cancer cells involves an ezrin-dependent crosstalk between G protein-coupled receptor 30 and estrogen receptor beta signaling. Steroids. 2016;111:113-20.
27. Tan A, Dang Y, Chen G, Mo Z. Overexpression of the fat mass and obesity associated gene (FTO) in breast cancer and its clinical implications. Int J Clin Exp Pathol. 2015;8(10):13405-10.
28. Su R, Dong L, Li C, Nachtergaele S, Wunderlich M, Qing Y, et al. R-2HG Exhibits Anti-tumor Activity by Targeting FTO/m(6)A/MYC/CEBPA Signaling. Cell. 2018;172(1-2):90-105 e23.
29. Dominissini D, Moshitch-Moshkovitz S, Schwartz S, Salmon-Divon M, Ungar L, Osenberg S, et al. Topology of the human and mouse m6A RNA methylomes revealed by m6A-seq. Nature. 2012;485(7397):201-6.
30. Meyer KD, Saletore Y, Zumbo P, Elemento O, Mason CE, Jaffrey SR. Comprehensive analysis of mRNA methylation reveals enrichment in 3′ UTRs and near stop codons. Cell. 2012;149(7):1635-46.
31. Braicu C, Gulei D, Raduly L, Harangus A, Rusu A, Berindan-Neagoe I. Altered expression of miR-181 affects cell fate and targets drug resistance-related mechanisms. Mol Asp Med. 2019;70:90-105.
32. Yoo JO, Kwak SY, An HJ, Bae IH, Park MJ, Han YH. miR-181b-3p promotes epithelial-mesenchymal transition in breast cancer cells through Snail stabilization by directly targeting YWHAG. Biochim Biophys Acta. 2016;1863(7 Pt A):1601-11.
33. Wang L, Wang YX, Chen LP, Ji ML. Upregulation of microRNA-181b inhibits CCL18-induced breast cancer cell metastasis and invasion via the NF-kappaB signaling pathway. Oncol Lett. 2016;12(6):4411-8.
34. Kurozumi S, Yamaguchi Y, Kurosumi M, Ohira M, Matsumoto H, Horiguchi J. Recent trends in microRNA research into breast cancer with particular focus on the associations between microRNAs and intrinsic subtypes. J. Hum. Genet. 2017;62(1):15-24.
35. Gillingham AK, Munro S. The small G proteins of the Arf family and their regulators. Annu Rev Cell Dev Biol. 2007;23:579-611.
36. Garg S, Sharma M, Ung C, Tuli A, Barral DC, Hava DL, et al. Lysosomal trafficking, antigen presentation, and microbial killing are controlled by the Arf-like GTPase Arl8b. Immunity. 2011;35(2):182-93.
37. Rosa-Ferreira C, Munro S. Arl8 and SKIP act together to link lysosomes to kinesin-1. Dev Cell. 2011;21(6):1171-8.
38. Bagshaw RD, Callahan JW, Mahuran DJ. The Arf-family protein, Arl8b, is involved in the spatial distribution of lysosomes. Biochem. Biophys. Res. Commun. 2006;344(4):1186-91.
39. Rosa-Ferreira C, Sweeney ST, Munro S. The small G protein Arl8 contributes to lysosomal function and long-range axonal transport in Drosophila. Biol Open. 2018;7(9).
40. Schiefermeier N, Scheffler JM, de Araujo ME, Stasyk T, Yordanov T, Ebner HL, et al. The late endosomal p14-MP1 (LAMTOR2/3) complex regulates focal adhesion dynamics during cell migration. J Cell Biol. 2014;205(4):525-40.
41. Hamalisto S, Jaattela M. Lysosomes in cancer-living on the edge (of the cell). Curr Opin Cell Biol. 2016;39:69-76.
42. Steffan JJ, Williams BC, Welbourne T, Cardelli JA. HGF-induced invasion by prostate tumor cells requires anterograde lysosome trafficking and activity of Na+-H+ exchangers. J Cell Sci. 2010;123(Pt 7):1151-9.
43. Pu J, Schindler C, Jia R, Jarnik M, Backlund P, Bonifacino JS. BORC, a multisubunit complex that regulates lysosome positioning. Dev Cell. 2015;33(2):176-88.
44. Rafn B, Nielsen CF, Andersen SH, Szyniarowski P, Corcelle-Termeau E, Valo E, et al. ErbB2-driven breast cancer cell invasion depends on a complex signaling network activating myeloid zinc finger-1-dependent cathepsin B expression. Mol Cell. 2012;45(6):764-76.
45. Dykes SS, Gray AL, Coleman DT, Saxena M, Stephens CA, Carroll JL, et al. The Arf-like GTPase Arl8b is essential for three-dimensional invasive growth of prostate cancer in vitro and xenograft formation and growth in vivo. Oncotarget. 2016;7(21):31037-52.

SUPPORTING INFORMATION

Additional supporting information may be found online in the Supporting Information section at the end of the article.

How to cite this article: Xu Y, Ye S, Zhang N, et al. The FTO/miR-181b-3p/ARL5B signaling pathway regulates cell migration and invasion in breast cancer. *Cancer Commun*. 2020;1–17. https://doi.org/10.1002/cac2.12075